

LOW-MEMORY END-TO-END TRAINING FOR ITERATIVE JOINT SPEECH DEREVERBERATION AND SEPARATION WITH A NEURAL SOURCE MODEL

Kohei Saijo^{1,2}, Robin Scheibler²

¹Department of Communications and Computer Engineering, Waseda University, Tokyo, Japan

²LINE Corporation, Tokyo, Japan

ABSTRACT

We propose an end-to-end framework for training iterative multi-channel joint dereverberation and source separation with a neural source model. We combine the unified dereverberation and separation update equations of ILRMA-T with a deep neural network (DNN) serving as source model. The weights of the model are directly trained by gradient descent with a permutation invariant loss on the output time-domain signals. One drawback of this approach is that backpropagation consumes memory linearly in the number of iterations. This severely limits the number of iterations, channels, or signal lengths that can be used during training. We introduce demixing matrix checkpointing to bypass this problem, a new technique that reduces the total memory cost to that of a single iteration. In experiments, we demonstrate that the introduced framework results in high-performance in terms of conventional speech quality metrics and word error rate. Furthermore, it generalizes to number of channels unseen during training.

Index Terms— Source separation, dereverberation, memory-efficient gradient computation, deep neural network

1. INTRODUCTION

The quality of speech signals recorded by microphones is generally degraded by interference, background noise, and reverberation. Source separation and dereverberation techniques have been eagerly studied as pre-processing for speech systems, e.g., automatic speech recognition (ASR). On the one hand, blind source separation (BSS) such as independent component analysis (ICA) [1], independent vector analysis (IVA) [2], independent low-rank matrix analysis (ILRMA) [3], dereverberation techniques such as weighted prediction error (WPE) [4], and their joint optimization such as ILRMA-T [5] have been a hot topic. On the other hand, supervised learning of deep neural networks (DNNs) has been shown to give significantly higher performance [6, 7]. In the multi-channel setup, beamforming with DNN-based time-frequency (TF) masking has been intensively studied and achieves high separation performance [8–10]. Recently, exploiting a pre-trained DNN as a source model for an iterative BSS algorithm was proposed and improved separation performance compared to conventional BSS [11]. Furthermore, end-to-end training by gradient descent of an iterative BSS algorithm with a source model DNN was demonstrated, leading to more accurate separation than conventional methods [12]. Computing the gradient of such an algorithm, even through multiple iterations, is made relatively easy by automatic differentiation, implemented via backpropagation (BP) in software such as Pytorch [13]. However, memory usage increases

linearly with the number of iterations because BP stores all the intermediate values of the computations.

The memory cost of BP becomes a bottleneck when using networks with deep layers or performing iterative computations. In prior work, reversible networks [14, 15] and checkpointing techniques [16] have been proposed to reduce the cost of storing the intermediate results. In the former, the activation of each layer can be completely reconstructed from the next layer’s, which enables to compute the gradient without storing any activation of hidden layers. In the latter, only a minimal number of intermediate results is stored and the remaining results are reconstructed from them.

In this work, we propose memory-efficient end-to-end training of a source model DNN for iterative joint dereverberation and separation. Specifically, the DNN estimates the TF mask of each source at each iteration. For the spatial and reverberation model updates, we use the inverse free update rules *time-decorrelation iterative source steering* (T-ISS) [17]. We evaluate two loss functions, scale-invariant [18] and convolutive transfer function invariant [19] signal-to-distortion ratios (SI-SDR and CI-SDR, respectively). The CI-SDR was recently shown to be effective for multi-channel enhancement [10]. To reduce the memory cost of iterative computation, we propose a new memory-efficient gradient computation technique, *demixing matrix checkpointing* (DMC), where the memory cost is nearly constant regardless of the number of iterations. Because the separated signals are computed with the demixing matrices, we can reconstruct all the intermediate results from them. We execute the forward pass without backpropagation, but store all the intermediate separation matrices. They are then used in the backward pass to reconstruct the intermediate separation results. We replay them in reverse order, and use BP to compute the gradient one iteration at a time. For a visual, skip to Fig. 1. The cost of storing the demixing matrices is negligible compared to maintaining the computational graph required by regular BP. DMC can be applied to any determined iterative source separation or dereverberation algorithm.

The key contributions of this work are summarized as follows.

1) This is the first work to train a source model DNN in joint dereverberation and separation framework. We show the superiority of our proposed method to conventional models [17], neural beamforming [8], and cascade connection of dereverberation [20] and separation [12] with source model DNNs. Specifically, the proposed method achieves improvements of 2.6 dB SDR, 0.2 PESQ, and reduction of WER by 20.1 % compared to the next best method. 2) We propose a memory-efficient gradient computation technique to train source model DNNs through multiple iterations. This technique can be applied to any determined source separation or dereverberation methods with iterative computations. Practically, for training with 20 iterations, the required memory is reduced from 31 GB (BP) to just 3 GB (DMC). Unexpectedly, we found out that despite running the forward pass twice, DMC was faster than BP, due to avoiding the

This work was done while Kohei Saijo was an intern at LINE Corporation.

overhead of maintaining the computational graph.

2. BACKGROUND

Assuming N sources are captured by M microphones, the microphone input signal in the short-time Fourier transform (STFT) domain is modeled auto-regressively, namely,

$$\mathbf{x}_{f,t} = \mathbf{A}_f \mathbf{s}_{f,t} + \sum_{l=D}^{D+L-1} \mathbf{Z}_{f,l} \mathbf{x}_{f,t-l}, \quad (1)$$

where $\mathbf{s}_{f,t}$ is the clean sources vector, $\mathbf{A}_f \in \mathbb{C}^{M \times N}$ the mixing matrix, and $\mathbf{Z}_{f,l}$ produces the reverberation component from past samples. L is the tap length and D is the delay to separate the desired signal and reverberation. $f = 1, \dots, F$ and $t = 1, \dots, T$ are the frequency bin and the time frame index in STFT-domain. We can rewrite (1) as

$$\mathbf{x}_{f,t} = \mathbf{A}_f \mathbf{s}_{f,t} + \bar{\mathbf{Z}}_f \bar{\mathbf{x}}_{f,t}, \quad (2)$$

where $\bar{\mathbf{Z}}_f = [\mathbf{Z}_{f,D}, \dots, \mathbf{Z}_{f,D+L-1}] \in \mathbb{C}^{N \times NL}$ and $\bar{\mathbf{x}}_{f,t} = [\mathbf{x}_{f,t-D}^\top, \dots, \mathbf{x}_{f,t-D-L+1}^\top]^\top \in \mathbb{C}^{NL}$. Supposing we know $\mathbf{W}_f = \mathbf{A}_f^{-1}$, i.e., the demixing matrix, and $\bar{\mathbf{Z}}_f$, we recover

$$\mathbf{s}_{f,t} = \mathbf{W}_f (\mathbf{x}_{f,t} - \bar{\mathbf{Z}}_f \bar{\mathbf{x}}_{f,t}). \quad (3)$$

Note that we focus on the determined case, i.e., $M = N$. In the following, \mathbf{I} and \mathbf{e}_n denote the identity matrix and the n -th canonical basis vector, and $^\top$ and H denote the transpose and Hermitian transpose of vectors or matrices.

Since conventional dereverberation methods such as WPE [4] assumes the existence of only one source, the cascade connection of dereverberation and separation is not optimal. To circumvent this problem, a *joint* dereverberation and separation framework was introduced as part of ILRMA-T [5]. The estimated clean sources vector, $\mathbf{y}_{f,t}$, is obtained by a unified filter $\mathbf{P}_f = \mathbf{W}_f [\mathbf{I}, -\bar{\mathbf{Z}}_f] \in \mathbb{C}^{N \times N(L+1)}$ as $\mathbf{y}_{f,t} = \mathbf{P}_f \tilde{\mathbf{x}}_{f,t}$ where $\tilde{\mathbf{x}}_{f,t} = [\mathbf{x}_{f,t}^\top, \bar{\mathbf{x}}_{f,t}^\top]^\top \in \mathbb{C}^{N(L+1)}$. The unified filter coefficients can be estimated by iteratively solving the following cost function [5],

$$\mathcal{J} = \sum_{f,t} \left[-2 \log |\det \mathbf{W}_f| + \frac{1}{T} \sum_n u_{f,t}(\mathbf{Y}_n) |\mathbf{p}_{n,f}^H \tilde{\mathbf{x}}_{f,t}|^2 \right], \quad (4)$$

where $(\mathbf{Y}_n)_{f,t} = (\mathbf{y}_{f,t})_n$. In ILRMA-T [5], $r_{n,f,t} = 1/u_{f,t}(\mathbf{Y}_n)$ corresponds to the low-rank non-negative source model [3]. To avoid the large matrix inversions in the update rule derived from iterative projection algorithm [5, 21], the inverse-free, rank-1 update rules, T-ISS have been proposed [17, 22]. The rank-1 corrections of T-ISS are applied in order to \mathbf{P} (frequency index is omitted). For $1 \leq n \leq N$,

$$\mathbf{P} \leftarrow \mathbf{P} - \mathbf{v}_n \mathbf{p}_n^H, \quad (5)$$

where \mathbf{p}_n^H is the n -th row vector of \mathbf{P} and $\mathbf{v}_n = [v_{1,n}, \dots, v_{N,n}]^\top$ is chosen to minimize (4), which yields,

$$v_{m,n} = \begin{cases} 1 - (\frac{1}{T} \sum_t u_{f,t}(\mathbf{Y}_n) |y_{n,f,t}|^2)^{-\frac{1}{2}}, & \text{if } m = n, \\ \frac{\sum_t u_{f,t}(\mathbf{Y}_m) y_{m,f,t} y_{n,f,t}^*}{\sum_t u_{f,t}(\mathbf{Y}_m) |y_{n,f,t}|^2}, & \text{otherwise.} \end{cases} \quad (6)$$

For $n > N$, the update becomes $\mathbf{P} \leftarrow \mathbf{P} - \mathbf{v}_n \mathbf{e}_n^\top$ and $v_{m,n}$ is,

$$v_{m,n} = \frac{\sum_t u_{f,t}(\mathbf{Y}_m) y_{m,f,t} \tilde{x}_{n,f,t}^*}{\sum_t u_{f,t}(\mathbf{Y}_m) |\tilde{x}_{n,f,t}|^2}, \quad (7)$$

where $\tilde{x}_{n,f,t}$ is the n -th component of $\tilde{\mathbf{x}}_{f,t}$.

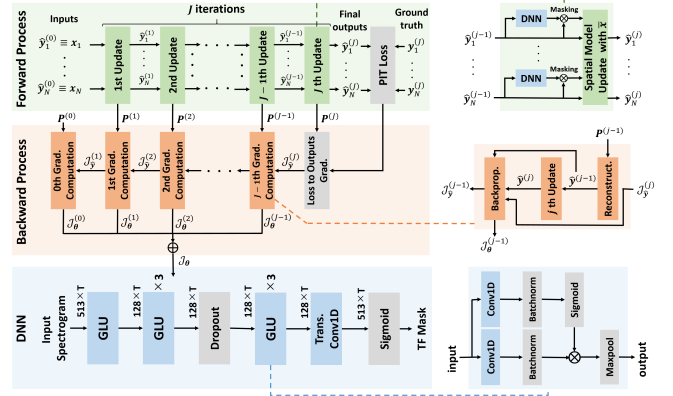


Fig. 1. Overview of our proposed method. We train a source model DNN (blue) directly through J iterations with a memory-efficient gradient computation. Unified filter $\mathbf{P}^{(j)}$ is stored in the forward pass (green) and used to reconstruct the separated signals in the backward pass (orange). The gradient to update the DNN parameter \mathcal{J}_θ is simply obtained by summing up the gradient at each iteration.

3. MEMORY-EFFICIENT SOURCE MODEL LEARNING

Conventionally, $u_{f,n}(\mathbf{Y}_m)$ in (4) is derived from a probabilistic model of speech. Instead, we propose to replace it altogether by a DNN and learn its weights by gradient descent. The loss function is directly applied to the time-domain output of multiple iterations of T-ISS. Although running BP through multiple iterations of such an algorithm has been successfully demonstrated before [12], the memory cost linearly increases with the number of iterations. One way to think about it is that BP unfolds the iterations into a very deep network. As an alternative to BP, we propose a gradient computation technique whose memory usage hardly increases regardless of the number of iterations. The overview of our proposed method is shown in Fig. 1.

3.1. Network Architecture

The network architecture, i.e., $u_{f,n}(\mathbf{Y})$, is shown at the bottom of Fig. 1. It consists of multiple gated linear units (GLU) [23] and one transpose convolution layer, all with kernel size three. The input is downsampled in the first block and then fed into six GLU blocks, with a dropout layer between the third and the fourth. Finally, the transpose convolution layer upsamples the input to the same size as the input and a TF mask is output. The mask may be understood as hiding the target source in the current source spectrogram estimate.

3.2. Loss Functions

We consider two time-domain loss functions, SI-SDR loss [18], and CI-SDR loss [19]. The former is a frequently used loss function [7]. The latter has been recently reported to be beneficial in multi-channel reverberant scenarios [10] because SI-SDR produces some strange artifacts in such scenarios [24]. In CI-SDR, a $K = 512$ tap filter $\alpha \in \mathbb{R}^K$ is utilized to make the SDR short-impulse-response-invariant. Let the estimated and groundtruth time-domain signals be $\hat{\mathbf{s}}$ and $\mathbf{s} \in \mathbb{R}^I$, respectively. Further define a matrix containing K shifts of \mathbf{s} in its columns, i.e., $\bar{\mathbf{S}} = [\bar{\mathbf{s}}_1, \dots, \bar{\mathbf{s}}_I]^\top \in \mathbb{R}^{I \times K}$, with i th row $\bar{\mathbf{s}}_i = [s_{i-1}, \dots, s_{i-K}]^\top \in \mathbb{R}^K$ where $i = 1, \dots, I$ is the time

Algorithm 1 Gradient Computation with DMC**Input :** Stored filter \mathbf{P} , Input signal $\tilde{\mathbf{x}}$, Loss E , Model parameter θ **Output:** Gradient to update model parameters \mathcal{J}_θ

```

1:  $\mathcal{J}_y^{(J)} \leftarrow \frac{\partial E}{\partial \hat{\mathbf{y}}^{(J)}}$   $\triangleright$  Gradient between loss and final output
2:  $\mathcal{J}_\theta \leftarrow \mathbf{0}$ 
3: for  $j \leftarrow J \dots 2, 1$  do
4:    $\hat{\mathbf{y}}^{(j-1)} \leftarrow \mathbf{P}^{(j-1)} \tilde{\mathbf{x}}$   $\triangleright$  Reconstruct  $j$ -1th separated signals
5:    $\hat{\mathbf{y}}^{(j)} \leftarrow \text{ISSupdate}(\hat{\mathbf{y}}^{(j-1)}, \theta)$ 
6:    $\mathcal{J}_y^{(j-1)}, \mathcal{J}_\theta^{(j-1)} \leftarrow \text{BackProp}(\mathcal{J}_y^{(j)}, \hat{\mathbf{y}}^{(j)}, \hat{\mathbf{y}}^{(j-1)}, \theta)$ 
7:    $\mathcal{J}_\theta \leftarrow \mathcal{J}_\theta + \mathcal{J}_\theta^{(j-1)}$ 

```

Table 1. Average CI-SDR of the best model among ten trials (different seeds) evaluated with 2 / 3 / 4ch. test set.

Metric	BP	DMC
CI-SDR (dB)	11.41 / 8.76 / 6.96	11.34 / 8.79 / 6.81

index. Then, the CI-SDR loss is

$$L_{\text{CISDR}} = -10 \log_{10} \left(\frac{\|\tilde{\mathbf{S}}\alpha\|^2}{\|\tilde{\mathbf{S}}\alpha - \hat{\mathbf{s}}\|^2} \right), \quad (8)$$

where and $\alpha = (\tilde{\mathbf{S}}^\top \tilde{\mathbf{S}})^{-1} \tilde{\mathbf{S}}^\top \hat{\mathbf{s}}$. The SI-SDR loss is also given by (8), but with $K = 1$.

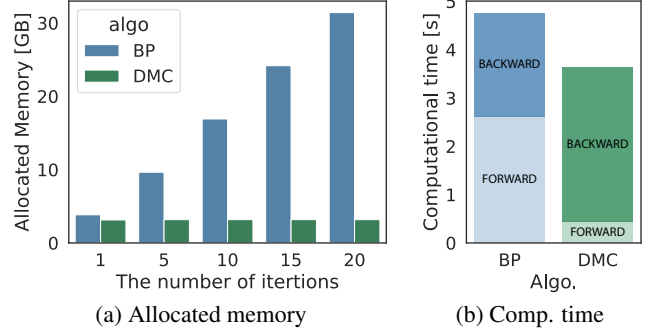
3.3. Demixing Matrix Checkpointing

The most commonly used method for gradient computation, BP, needs not only the final output but all the intermediate results. It starts from the final loss and works its way backward through the computational graph computing the gradient along the way. Thus, memory cost is a bottleneck for iterative computations. However, by storing the demixing matrices during the forward pass, we can recreate the intermediate separation results. This makes it possible to compute the gradient one iteration at a time during the backward pass without storing anything besides the demixing matrices. Based on this idea, we propose a new memory-efficient gradient computation technique, demixing matrix checkpointing (DMC). Pseudocode for DMC is shown in Algorithm 1. This reduces the memory requirements to that of a single iteration and of storing the matrices. The number of values in the latter is $F \times (L + 1) \times M^2 \times J$, where J denotes the number of iterations. Using realistic values for the parameters, e.g., $F = 513$, $L = 5$, $M = 2$, and $J = 20$, and 32bit floating-point precision, the required memory is less than 1 MB.

DMC proceeds by computing the contribution of each iteration to the gradient in reverse order. At the j -th iteration, we first reconstruct the separated signals of the previous iteration $\hat{\mathbf{y}}^{(j-1)}$ using the unified filter $\mathbf{P}^{(j-1)}$ stored during the forward pass. Then, we re-compute $\hat{\mathbf{y}}^{(j)}$ in the same way as the forward pass. The gradient of the model parameter at j -th iteration, $\mathcal{J}_\theta^{(j-1)}$, is computed by BP. Considering the same DNN is used in all the iterations, i.e., the DNN parameters are shared, the gradient to update the DNN parameters, \mathcal{J}_θ , is simply obtained by summing up $\mathcal{J}_\theta^{(j)}$ for all the iterations.

4. EXPERIMENTS

There are several goals for our experiments. First, we assess the performance of DMC compared to BP. Even small numerical differences in the gradient computation quickly lead to different trajectories of stochastic gradient descent, and, ultimately, different

**Fig. 2.** (a) Allocated memory of BP and DMC measured using `nvidia-smi` command. (b) Computational time of BP and DMC for forward and backward pass, where batch size is 8.

weights. Therefore, to confirm that training with DMC and BP lead to similar outcomes, we train one model with each for 10 different random seeds and compare those with the best validation score. Second, we measure the memory cost and runtime of both methods. Finally, we evaluate the performance of the proposed joint speech dereverberation and separation with a source model DNN trained using this method. The evaluation metrics are CI-SDR, SI-SDR, scale-invariant signal-to-interference ratio (SI-SIR), the short-time objective intelligibility (STOI) [25], the perceptual evaluation of speech quality (PESQ) [26], speech-to-reverberation modulation energy ratio (SRMR) [27], and word error rate (WER) of an ASR system trained using the `wsj/asr1` recipe from the ESPNet framework [28]. Since the same source model is used for each source to be separated, and the spatial model update has no trainable parameters, our proposed method can be applied regardless of the number of speakers. To demonstrate this, we train the model on 2 channels mixtures, but test on 2, 3, and 4 channels mixtures. The baselines are as follows. **ILRMA-T-ISS** [17]: T-ISS with low-rank non-negative source model [3]. It has no trainable parameters and performs joint dereverberation and separation blindly. **Cascade connection of DNN-WPE and DNN-AuxIVA-ISS** [12, 20]: Cascade method of WPE and AuxIVA-ISS with source model DNNs. The DNN parameters of WPE and AuxIVA are not shared. Training is done end-to-end. **DNN-based MVDR beamforming** [10]: MVDR beamforming with DNN-based TF masking. Here, we use the BLSTM-based DNN from [10] rather than that shown in Fig. 1.

4.1. Dataset

We use the simulated reverberant noisy mixtures dataset introduced in [12]. It consists of speech from the WSJ1 corpus [29] and noise from the CHIME3 dataset [30]. The reverberation times were chosen randomly from 200 ms to 600 ms. Compared to [12], the only difference is that we removed the DC-offset by subtracting from itself the mean value of each speech sample. The number of speech sources is the same as that of microphones (determined case). The relative power of sources was chosen randomly from -5 dB to 5 dB. The noise was scaled to attain an SNR between 10 dB to 30 dB. Training, validation, and test sets contain 37416, 503, and 333 mixtures, respectively. WER for the clean, anechoic test set is 9.25% .

4.2. Experimental Setup

We trained DNNs using only mixtures of two speakers. The batch size was 8 and the length of input signal was 7 seconds. For STFT,

Table 2. Average CI-SDR, SI-SDR and SI-SIR in decibels, and STOI, PESQ, SRMR and WER of separated signals from the test set. Source model DNNs are trained using only 2ch. data and evaluated using 2, 3, and 4ch. data. The proposed method is indicated by a star (*).

Ch.	Algo.	Model	Loss	CI-SDR \uparrow	SI-SDR \uparrow	SI-SIR \uparrow	STOI \uparrow	PESQ \uparrow	SRMR \uparrow	WER \downarrow
2	Obs.	-	-	-0.4	-2.1	0.0	0.728	1.208	5.13	111.4%
	MVDR	BLSTM	CI-SDR	5.5	-2.5	26.7	0.824	1.578	6.41	68.3%
	WPE+AuxIVA	GLU	CI-SDR	9.7	4.7	23.3	0.878	1.586	6.53	54.3%
	T-ISS	NMF	-	7.9	2.7	24.4	0.860	1.552	6.45	49.3%
	T-ISS*	GLU	SI-SDR	11.3	6.6	28.3	0.909	1.722	6.70	31.7%
	T-ISS*	GLU	CI-SDR	12.3	6.1	28.3	0.907	1.783	6.87	29.2%
3	Obs.	-	-	-3.6	-5.0	-3.3	0.640	1.137	4.58	145.9%
	WPE+AuxIVA	GLU	CI-SDR	7.8	3.7	19.9	0.849	1.462	6.36	73.4%
	T-ISS	NMF	-	4.4	-0.7	16.0	0.799	1.371	6.16	77.9%
	T-ISS*	GLU	SI-SDR	9.2	5.5	23.3	0.884	1.577	6.59	45.8%
	T-ISS*	GLU	CI-SDR	9.7	5.0	23.0	0.879	1.617	6.65	43.8%
4	Obs.	-	-	-5.4	-6.8	-5.3	0.584	1.122	4.12	162.8%
	WPE+AuxIVA	GLU	CI-SDR	6.4	2.5	17.4	0.824	1.387	6.21	87.7%
	T-ISS	NMF	-	2.0	-3.0	11.3	0.755	1.284	5.81	98.1%
	T-ISS*	GLU	SI-SDR	7.5	4.1	19.8	0.859	1.471	6.31	58.5%
	T-ISS*	GLU	CI-SDR	7.7	3.5	19.4	0.849	1.502	6.40	57.3%

we used a Hann window with the size of 1024, and hop size was 256. We set the number of iterations of T-ISS and AuxIVA-ISS to 20 in training, and 50, 75 and 100 for 2, 3 and 4 channel mixtures in test. Note that the number of iterations for DNN-WPE was set to 1 both in training and test following [20]. The delay D was set to 1 in the T-ISS, and 3 in WPE because such setting gave the best performance. Both use $L = 5$ taps. To solve the scale and phase ambiguity, we applied projection back [31] to the final output.

All the algorithms are implemented in Pytorch [13]. Allocated memory and computational time were measured with the `nvidia-smi` command and the profiler of Pytorch [13], respectively. Experiments were conducted on a Linux workstation with an Intel® Xeon® Gold 6230 CPU 2.10 GHz with 8 cores, an NVIDIA® Tesla® V100 graphical processing unit (GPU), and 64 GB of RAM.

4.3. Results

We start by summarizing the results of comparing BP and DMC. To measure the numerical difference between the two, we computed the gradients for 500 samples. We confirmed that the difference between the two is never more than 0.05 % of the norm of BP’s gradient (with 32 bit precision). We conclude that both methods compute the same gradients up to numerical precision. Table 1 shows the test CI-SDR of the best models obtained from training with BP and DMC for 10 different random seeds on a reduced dataset of 2048 samples. The performance obtained with both training methods is remarkably close and we conclude that DMC correctly computes the gradient.

Fig. 2 shows the memory used as a function of the number of iterations, and runtimes of the forward and backward passes per batch of 8 samples. While BP consumes memory linearly proportional to the number of iterations, the memory cost of DMC is essentially constant. Under the setting of our experiment, i.e., 20 iterations, DMC used only about a tenth of the memory of BP. In addition, surprisingly, even though the backward of DMC is obviously slower due to the necessity of reconstructing the separated signals and re-running the forward pass, DMC was found to be faster than BP in the total of the forward and the backward passes. This means that in our case the cost of the forward pass is less than the overhead created by the computational graph needed by BP.

Finally, we turn to the evaluation of the joint dereverberation and separation itself. Table 2 shows the evaluation results on the test

set. Our proposed method, i.e., T-ISS with the GLU source model (marked with a *), outperforms all the baseline methods on all metrics when trained with either SI-SDR or CI-SDR loss, as well as on 3 and 4 channels. Especially, training with CI-SDR loss gave the best WER. Compared to the cascade connection of DNN-WPE and DNN-AuxIVA-ISS, the proposed method achieves much higher performance. Furthermore, even though the cascade method includes two sophisticated trained DNNs, its WER in 2ch. data was worse than conventional T-ISS that uses zero trainable parameters. The lower SI-SIR of the cascade method and the fact that the speech recognition results contained a lot of insertion errors imply that the separation in the cascade method was not successful. This confirms the effectiveness of performing jointly the dereverberation and separation, rather than separately. We note that this was not the case for three and four channels, where the conventional NMF source model struggled more than the cascade with trained models (although admittedly neither gave great results there).

5. CONCLUSION

We proposed to learn a source model for joint dereverberation and separation with memory-efficient gradient computation via DMC. We trained a source model DNN end-to-end through multiple iterations. While the memory cost of BP increases in proportion to the number of iterations, that of DMC is nearly constant by removing the need to store the computational graph during the forward pass. We evaluated two losses, SI-SDR and CI-SDR, of which the latter gave the best results. In experiments, DMC was found to be capable of learning at comparable performance with lower memory costs and computational time than BP. Our proposed method achieved much higher performance, especially when trained with CI-SDR loss, than conventional joint dereverberation and separation method and their cascade connection with neural source models. These results all confirm the effectiveness of the joint optimization of dereverberation and separation with trained neural source models.

6. REFERENCES

- [1] P. Comon, “Independent component analysis, a new concept?,” *Signal Processing*, vol. 36, no. 3, pp. 287–314, 1994.
- [2] T. Kim, T. Eltoft, and T.-W. Lee, “Independent vector analysis: An extension of ica to multivariate components,” in *Advances in Cryptology - ASIACRYPT2016*. 2006, pp. 165–172, Springer Berlin Heidelberg.
- [3] D. Kitamura, N. Ono, H. Sawada, H. Kameoka, and H. Saruwatari, “Determined blind source separation unifying independent vector analysis and nonnegative matrix factorization,” *IEEE/ACM Trans. Audio Speech Lang. Process.*, vol. 24, no. 9, pp. 1626–1641, 2016.
- [4] T. Nakatani, T. Yoshioka, K. Kinoshita, M. Miyoshi, and B.-H. Juang, “Speech dereverberation based on variance-normalized delayed linear prediction,” *IEEE Trans. Audio Speech Lang. Process.*, vol. 18, no. 7, pp. 1717–1731, 2010.
- [5] R. Ikeshita, N. Ito, T. Nakatani, and H. Sawada, “A unifying framework for blind source separation based on a joint diagonalizability constraint,” in *Proc. IEEE EUSIPCO*, 2019, pp. 1–5.
- [6] D. Yu, M. Kolbæk, Z. H. Tan, and J. Jensen, “Permutation invariant training of deep models for speaker-independent multi-talker speech separation,” in *Proc. IEEE ICASSP*, 2017, pp. 241–245.
- [7] Y. Luo and N. Mesgarani, “Tasnet: Time-domain audio separation network for real-time, single-channel speech separation,” in *Proc. IEEE ICASSP*, 2018, pp. 696–700.
- [8] J. Heymann, L. Drude, and R. Haeb-Umbach, “Neural network based spectral mask estimation for acoustic beamforming,” in *Proc. IEEE ICASSP*, 2016, pp. 196–200.
- [9] T. Ochiai, S. Watanabe, T. Hori, and J. R. Hershey, “Multi-channel end-to-end speech recognition,” in *Proc. ICML*, 2017, p. 2632–2641.
- [10] C. Boeddeker et al., “Convolutional transfer function invariant sdr training criteria for multi-channel reverberant speech separation,” in *Proc. IEEE ICASSP*, 2021, pp. 8428–8432.
- [11] N. Makishima et al., “Independent deeply learned matrix analysis for determined audio source separation,” *IEEE/ACM Trans. Audio Speech Lang. Process.*, vol. 27, no. 10, pp. 1601–1615, 2019.
- [12] R. Scheibler and M. Togami, “Surrogate source model learning for determined source separation,” in *Proc. IEEE ICASSP*, 2021, pp. 176–180.
- [13] Adam Paszke et al., “Pytorch: An imperative style, high-performance deep learning library,” in *Advances in Neural Information Processing Systems*, H. Wallach, H. Larochelle, A. Beygelzimer, F. d’Alché-Buc, E. Fox, and R. Garnett, Eds. 2019, vol. 32, Curran Associates, Inc.
- [14] A. N. Gomez, M. Ren, R. Urtasun, and R. B. Grosse, “The reversible residual network: Backpropagation without storing activations,” in *Proceedings of the 31st International Conference on Neural Information Processing Systems*, Red Hook, NY, USA, 2017, NIPS’17, pp. 2211–2221.
- [15] M. E. Sander, P. Ablin, M. Blondel, and G. Peyré, “Momentum residual neural networks,” in *Proc. ICML*, 2021, pp. PMLR 139:9276–9287.
- [16] J. Martens and I. Sutskever, *Training Deep and Recurrent Networks with Hessian-Free Optimization*, pp. 479–535, Springer Berlin Heidelberg, Berlin, Heidelberg, 2012.
- [17] T. Nakashima, R. Scheibler, M. Togami, and N. Ono, “Joint dereverberation and separation with iterative source steering,” in *Proc. IEEE ICASSP*, 2021, pp. 216–220.
- [18] J. L. Roux, S. Wisdom, H. Erdogan, and J. R. Hershey, “Sdr – half-baked or well done?,” in *Proc. IEEE ICASSP*, 2019, pp. 626–630.
- [19] E. Vincent, R. Gribonval, and C. Fevotte, “Performance measurement in blind audio source separation,” *IEEE Trans. Audio Speech Lang. Process.*, vol. 14, no. 4, pp. 1462–1469, June 2006.
- [20] K. Kinoshita, M. Delcroix, Haeyong Kwon, Takuma Mori, and T. Nakatani, “Neural network-based spectrum estimation for online wpe dereverberation,” in *Proc. ISCA INTERSPEECH*, 2017.
- [21] N. Ono, “Stable and fast update rules for independent vector analysis based on auxiliary function technique,” in *Proc. IEEE WASPAA*, 2011, pp. 189–192.
- [22] R. Scheibler and N. Ono, “Fast and stable blind source separation with rank-1 updates,” in *Proc. IEEE ICASSP*, 2020, pp. 236–240.
- [23] Y. N. Dauphin, A. Fan, M. Auli, and D. Grangier, “Language modeling with gated convolutional networks,” in *Proc. ICML*, D. Precup and Y. W. Teh, Eds. Aug 2017, vol. 70 of *Proceedings of Machine Learning Research*, pp. 933–941, PMLR.
- [24] L. Drude, J. Heitkaemper, C. Bøddeker, and R. Haeb-Umbach, “Sms-wsj: Database, performance measures, and baseline recipe for multi-channel source separation and recognition,” 2019.
- [25] C. H. Taal, R. C. Hendriks, R. Heusdens, and J. Jensen, “An algorithm for intelligibility prediction of time–frequency weighted noisy speech,” *IEEE Trans. Audio Speech Lang. Process.*, vol. 19, no. 7, pp. 2125–2136, 2011.
- [26] A. W. Rix, J. G. Beerends, M. P. Hollier, and A. P. Hekstra, “Perceptual evaluation of speech quality (PESQ)—a new method for speech quality assessment of telephone networks and codecs,” in *Proc. IEEE ICASSP*, 2001, vol. 2, pp. 749–752.
- [27] T. H. Falk, C. Zheng, and W. Chan, “A non-intrusive quality and intelligibility measure of reverberant and dereverberated speech,” *IEEE Trans. Audio Speech Lang. Process.*, vol. 18, no. 7, pp. 1766–1774, 2010.
- [28] S. Watanabe et al., “ESPnet: End-to-end speech processing toolkit,” in *Proc. ISCA INTERSPEECH*, 2018, pp. 2207–2211.
- [29] Linguistic Data Consortium, and NIST Multimodal Information Group, *CSR-II (WSJ) Complete LDC94S13A*, Linguistic Data Consortium, Philadelphia, 1994, Web Download.
- [30] J. Barker, R. Marxer, E. Vincent, and S. Watanabe, “The third ‘chime’ speech separation and recognition challenge: Dataset, task and baselines,” in *Proc. IEEE ASRU*, 2015, pp. 504–511.
- [31] N. Murata, S. Ikeda, and A. Ziehe, “An approach to blind source separation based on temporal structure of speech signals,” *Neurocomputing*, vol. 41, no. 1, pp. 1–24, 2001.